nature communications



Article

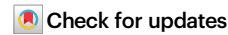
https://doi.org/10.1038/s41467-024-54960-1

Minimal presynaptic protein machinery governing diverse kinetics of calcium-evoked neurotransmitter release

Received: 23 March 2024

Accepted: 25 November 2024

Published online: 30 December 2024



Dipayan Bose^{1,2,6}, Manindra Bera © ^{1,3,6}, Christopher A. Norman © ^{4,5}, Yulia Timofeeva © ⁵, Kirill E. Volynski © ^{3,4} — & Shyam S. Krishnakumar © ^{1,2,4} —

Neurotransmitters are released from synaptic vesicles with remarkable precision in response to presynaptic calcium influx but exhibit significant heterogeneity in exocytosis timing and efficacy based on the recent history of activity. This heterogeneity is critical for information transfer in the brain, yet its molecular basis remains poorly understood. Here, we employ a biochemically-defined fusion assay under physiologically relevant conditions to delineate the minimal protein machinery sufficient to account for various modes of calcium-triggered vesicle fusion dynamics. We find that Synaptotagmin-1, Synaptotagmin-7, and Complexin synergistically restrain SNARE complex assembly, thus preserving vesicles in a stably docked state at rest. Upon calcium activation, Synaptotagmin-1 induces rapid vesicle fusion, while Synaptotagmin-7 mediates delayed fusion. Competitive binding of Synaptotagmin-1 and Synaptotagmin-7 to the same SNAREs, coupled with differential rates of calcium-triggered fusion clamp reversal, govern the overall kinetics of vesicular fusion. Under conditions mimicking sustained neuronal activity, the Synaptotagmin-7 fusion clamp is destabilized by the elevated basal calcium concentration, thereby enhancing the synchronous component of fusion. These findings provide a direct demonstration that a small set of proteins is sufficient to account for how nerve terminals adapt and regulate the calcium-evoked neurotransmitter exocytosis process to support their specialized functions in the nervous system.

Information transfer in the brain depends on the release of neurotransmitters stored in synaptic vesicles (SVs) within the presynaptic terminals. SV fusion with the presynaptic membrane and neurotransmitter release are tightly regulated by changes in the presynaptic Ca²⁺ concentration ([Ca²⁺]) and can occur in less than a millisecond after the action potential (AP) invades a presynaptic terminal^{1,2}. In addition to fast, synchronous release that keeps pace with APs, many synapses also exhibit delayed asynchronous release that persists for

tens to hundreds of milliseconds^{1,2}. Synapses also vary in terms of how the probability of neurotransmitter release is altered by the recent history of AP firing^{3,4}. The balance between synchronous and asynchronous release, and the degree of synaptic facilitation or depression of release, differs not only among neurons but also among synapses supplied by a single axon according to their postsynaptic targets. This heterogeneity is important in coordinating activity within neuronal networks⁵⁻⁷.

¹Nanobiology Institute, Yale University, West Haven, CT, USA. ²Department of Neurology, School of Medicine, Yale University, New Haven, CT, USA. ³Department of Cell Biology, School of Medicine, Yale University, New Haven, CT, USA. ⁴Department of Clinical and Experimental Epilepsy, UCL Queen Square Institute of Neurology, London, UK. ⁵Department of Computer Science, University of Warwick, Coventry, UK. ⁶These authors contributed equally: Dipayan Bose, Manindra Bera. — e-mail: k.volynski@ucl.ac.uk; shyam.krishnakumar@yale.edu

The key components of the synaptic vesicular exocytosis machinery have been identified^{1,2,8}. These include the SNARE proteins that catalyze SV fusion (VAMP2 on the SV, and Syntaxin/SNAP25 on the presynaptic membrane); Ca²⁺ release sensors that couple SV fusion to Ca²⁺ signal (Synaptotagmins); and proteins that regulate SV docking and the organization of vesicular release sites (e.g., Complexin (CPX). Munc13, Munc18). Ca²⁺-evoked neurotransmitter release occurs from a readily releasable pool (RRP) of vesicles docked at the presynaptic active zone^{1,2,9}. A consensus has emerged that, at an individual RRP vesicle, multiple SNARE complexes are arrested ('clamped') in a partially-assembled state (SNAREpins) by Synaptotagmins and CPX. Ca²⁺ activation of Synaptotagmins releases the fusion clamp allowing SNAREpins to fully assemble and drive SV fusion¹⁰⁻¹². Despite this general scheme, the reasons for variations in the synchrony of exocytosis or the occurrence of short-term facilitation or depression among synapses, remain poorly understood.

Synchronous neurotransmitter release, occurring within a few milliseconds of the arrival of an AP, is triggered by a transient high local $[Ca^{2+}]$ ($[Ca^{2+}]_{peak} \sim 10-100 \,\mu\text{M}$) at vesicular release sites, and genetic deletion and substitution experiments have shown that it requires a fast, low-affinity Ca²⁺ sensor such as Synaptotagmin 1, 2 or 9 (Syt1, Syt2, Syt9)^{13,14}. Asynchronous neurotransmitter release can occur in response to a single AP but is particularly prominent during and following high-frequency bursts of APs. This delayed release requires a persistent elevation of presynaptic [Ca²⁺] and this [Ca²⁺]_{residual} is thought to reach a low micromolar concentration^{1,15,16}. At many synapses, accumulation of [Ca2+]_{residual} also leads to transient facilitation of the fast synchronous release component^{1,4}. The slow, highaffinity Ca²⁺ sensor Synaptotagmin 7 (Syt7), which is activated by both [Ca²⁺]_{peak} and [Ca²⁺]_{residual}, has been implicated in regulating both asynchronous release and short-term facilitation^{17–20}. Indeed, previous studies have shown that genetic removal of Syt7 reduces short-term synaptic facilitation and asynchronous release^{13,18,19}. However, the Syt7's role in asynchronous release remains a topic of debate as other Ca2+-release sensors (e.g. Syt1, Syt3 and Doc2A) have also been implicated in mediating asynchronous release component 17,21-23.

An inherent limitation of genetic studies is their inability to demonstrate whether Syt1 and Syt7 alone are *sufficient* to regulate the timing and plasticity of neurotransmitter release, as the contribution of other presynaptic proteins cannot be ruled out. Furthermore, because vesicular exocytosis involves an interplay of presynaptic Ca²⁺ dynamics and Ca²⁺ sensors, a quantitative account of synchronous/ asynchronous release kinetics and short-term plasticity requires precise control and measurement of [Ca²⁺]. This is difficult to achieve in intact synapses owing to the small size of the active zone and the high speed of Ca²⁺ diffusion and buffering^{24,25}.

Hence, we sought to determine whether Syt1 and Syt7 (along with SNAREs and CPX) are sufficient to determine the kinetics and activity-dependent changes in Ca^{2+} -evoked SV release. Additionally, we aimed to uncover the underlying molecular mechanisms governing the cooperative action of Syt1 and Syt7. To achieve this, we took a reductionistic approach of combining an in vitro reconstituted fusion assay^{26–29} with quantitative computational modeling¹². Specifically, we utilized a biochemically-defined high-throughput assay based on a suspended lipid membrane platform that uses fluorescence microscopy to track the docking, clamping (equivalent to the delay from docking to spontaneous fusion), and Ca^{2+} -triggered fusion of individual vesicles at tens of milliseconds precision. Critically, this setup allowed precise control over the identity and density of the included proteins, as well as the $[Ca^{2+}]$ signal^{26,28–30}.

We report that under resting conditions, Syt1 and Syt7 along with CPX clamp vesicle fusion to produce docked vesicles. Upon Ca²⁺-influx, Syt1 and Syt7 act as 'fast' and 'slow' release sensors respectively and govern the overall fusion kinetics by competitively binding to the same SNARE complex. Computational modeling suggests that the slower

Ca²⁺-triggered reversal of the Syt7 fusion clamp, in contrast to Syt1, accounts for the delayed fusion kinetics. When [Ca²⁺]_{basal} is elevated to mimic neuronal activity, Syt7 enhances Ca²⁺-synchronized vesicle fusion independent of Syt1, due to selective destabilization of the Syt7 clamp by elevated [Ca²⁺]_{basal}. In summary, our data suggest that Syt1, Syt7, SNAREs, and CPX constitute the minimal protein machinery necessary to support the diverse kinetics and activity-dependent dynamics of Ca²⁺-evoked neurotransmitter release.

Results

Recently, using the in vitro experimental setup, we demonstrated that under physiologically relevant conditions, Syt1 and CPX are sufficient to produce clamped (RRP-like) vesicles, and these stably docked vesicles can be triggered to fuse rapidly by Ca²⁺ addition³⁰. Building on this advance, we designed the reconstitution conditions to investigate the cooperative action of Syt1 and Syt7 as follows: in all experiments, we used small unilamellar vesicles containing VAMP2 and Syt1 and included CPX in the solution (Fig. 1a, Supplementary Fig. 1). We reconstituted pre-formed t-SNAREs (a 1:1 complex of Syntaxin1 and SNAP-25) and Syt7 (when warranted) in the suspended lipid membrane (Fig. 1a, Supplementary Fig. 1). We incorporated Syt7 in the suspended lipid membrane reflecting its predominant localization in the presynaptic membrane in central synapses^{31,32}. Since the concentration of Syt7 within the active zone is unknown and likely varies among different types of synapses, we tested the effect of varying Syt7 concentration. In all cases, we monitored large ensembles of vesicles (~150 - 200 vesicles) and used fluorescently labeled lipid (2% ATTO647N-PE), introduced in the vesicles to track the docking and fate of individual vesicles (Fig. 1a and Methods). To trigger the fusion of docked vesicles, we chose a [Ca²⁺] of 100 µM. This concentration aligns with the [Ca²⁺]_{peak} observed at presynaptic vesicular release sites²⁴ and is sufficient to saturate both Syt1 and Syt7¹⁰, therefore mitigating possible variability stemming from differential activation of Syt1 and Syt7.

Syt7 delays the fusion of Syt1-containing vesicles in a concentration-dependent manner

In the absence of Syt7, the majority (-95%) of the Syt1/VAMP2 containing vesicles that docked to the t-SNARE bilayers were 'immobile' and remained unfused during an initial 10 min observation window (Supplementary Fig. 2). Addition of Ca^{2+} triggered the fusion of -90% of the stably clamped vesicles within 5 s as measured by lipid mixing (Fig. 1b). Notably, a significant portion of fusion events (-70%) occurred within 2 frames (-300 ms) following the initial arrival of Ca^{2+} signal (Fig. 1b, c), even though the [Ca^{2+}] reached 100 μ M over time scale of -750 milliseconds (Supplementary Fig. 3).

Inclusion of Syt7 in the t-SNARE-containing bilayer (at concentrations ranging from 1:2000 to 1:200 protein-to-lipid ratio) had no discernable effect on the number or the fate of the docked Syt1/VAMP2 vesicles (Supplementary Fig. 2). Hence, the vast majority (~90%) of the vesicles remained stably docked in an immobile clamped state (Supplementary Fig. 2). Likewise, Syt7 did not impact the Ca²⁺-induced fusion competence as ~90% of the docked vesicles fused within 5 s following the addition of Ca²⁺ (100 μM) (Fig. 1b). However, we observed significant delays in the kinetics of Ca²⁺-triggered fusion, and these delays correlated with the amount of Syt7 included in the bilayer (Fig. 1c). The proportion of 'coupled release' i.e. vesicles undergoing fusion within 2 frames (~300 ms) following the initial arrival of Ca²⁺ signal progressively declined from approximately 70% to 10%, as the concentration of Syt7 in the bilayer was increased from 1:2000 to 1:200 (Fig. 1b, c). Noteworthy, this impact was specific to Syt7, as inclusion of Syt1 (instead of Syt7) in the suspended bilayer, even at a protein-tolipid ratio of 1:200, did not alter the likelihood or kinetics of Ca²⁺triggered fusion of Syt1/VAMP2 vesicles (Fig. 1b, c). Taken together, these data indicate that Syt7 influences the kinetics of Ca²⁺-triggered

fusion for Syt1/VAMP2 vesicles in a concentration-dependent manner, without altering the fusion competence of docked vesicles.

Contribution of Syt7 to the establishment of the fusion clamp

The clamping efficiency of docked vesicles was similar in the absence or presence of Syt7, with approximately 90% of docked vesicles stably clamped under both conditions (Supplementary Fig. 2). Therefore, it remained unclear whether Syt7 also contributes to the fusion clamp (in addition to Syt1 and CPX) under these conditions. Simple removal of Syt1 and/or CPX from the reaction mixture was not feasible, as omitting CPX potentiated spontaneous fusion, while leaving out Syt1 significantly reduced the number of docked vesicles, precluding any meaningful analysis^{26,30}. Hence, we developed reconstitution conditions specifically tailored to investigate the role of Syt7 as a fusion clamp.

In previous work, we demonstrated that CPX could be omitted under low VAMP2 copy number conditions (i.e. vesicles containing -13 copies of VAMP2 and -22 copies of Syt1), as Syt1 alone could produce stably clamped Ca²+-sensitive vesicles²7,30. We further showed that disrupting the Syt1-SNARE interaction at the 'primary' interface using the well-established mutations in the Syt1 C2B domain (R281A, E295A, Y338W, R398A, R399A; referred to as Syt1^Q)³3,34 specifically abrogates the Syt1 fusion clamp without affecting vesicle docking³0. Given this background, we investigated Syt7's impact on the fusion clamp by utilizing the Syt1^Q mutant in the CPX-free, low VAMP2 condition (i.e. Syt1^Q/VAMP2^{low} vesicles).

As anticipated, in the absence of Syt7, the majority (>90%) of docked Syt1^Q/VAMP2^{low} vesicles fused spontaneously. Inclusion of Syt7 in the bilayer restored the clamp on Syt1^Q/VAMP2^{low} vesicles in a dose-

dependent manner, with approximately 40% and 90% of vesicles remaining stably docked in an immobile state with Syt7 included at 1:800 and 1:200 (protein-to-lipid ratio) respectively (Fig. 2a). Furthermore, these stably docked vesicles could be triggered to fuse by the addition of $100\,\mu\text{M}$ Ca²+ (Fig. 2b), but the fusion kinetics were desynchronized from the Ca²+ signal, with a temporally distributed vesicle fusion pattern (Fig. 2c). This suggests that Syt7 can independently establish a calcium-sensitive fusion clamp and may act in conjunction with Syt1 and CPX under physiologically relevant conditions.

Syt1 and Syt7 regulate Ca²⁺-evoked fusion via competitive binding to the SNARE complex

Next, we investigated the impact of Ca²⁺-binding-deficient Syt1 and Syt7 mutants to understand the mechanisms behind their synergistic action (Fig. 3). Specifically, we employed Syt1 with D309A, D363A, D365A mutations in the C2B domain (Syt1^{DA}), and Syt7 with D225A, D227A, D233A, D357A, D359A mutations in the C2AB domains (Syt7^{DA}). The introduction of Ca²⁺-insensitive Syt7^{DA} in the bilayer resulted in a concentration-dependent reduction in Ca²⁺-evoked fusion of docked vesicles containing Syt1^{WT}/VAMP2, with ~30% decrease at a low (1:800 protein-to-lipid) and ~70% reduction at high (1:200) Syt7^{DA} concentrations (Fig. 3a). However, Syt7^{DA} had no discernable effect on the fusion kinetics, with the majority of vesicles fusing within the first 2 frames following Ca²⁺ arrival (Fig. 3a).

As expected, the disruption of Ca²⁺ binding to Syt1 (Syt1^{DA}) eliminated Ca²⁺-triggered vesicular fusion (-7%) without altering the docking or clamping of the vesicles. However, the inclusion of Syt7^{WT} into the bilayer restored Ca²⁺-evoked fusion to levels corresponding with the concentration of Syt7^{WT} in the bilayer (-40% and -75% with

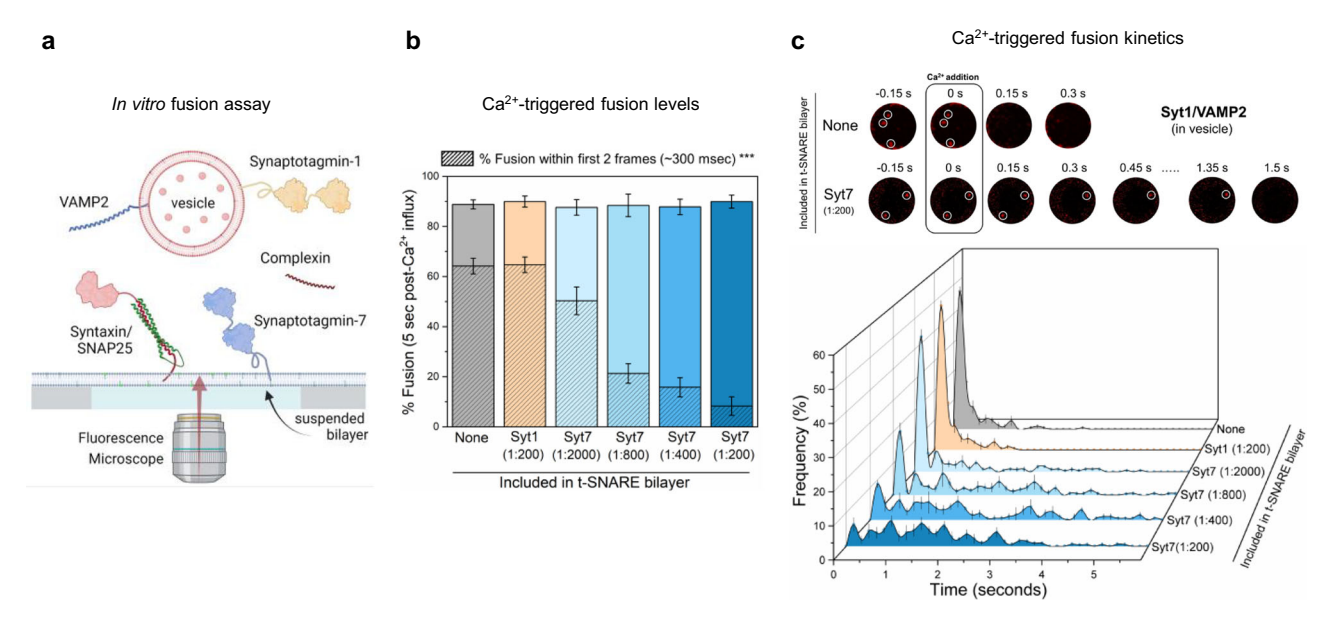


Fig. 1 | **Impact of Syt7 on Ca²⁺-evoked fusion of Syt1/VAMP2 vesicles. a** In a typical in vitro fusion experiment, vesicles containing VAMP2 (-70 copies) and Syt1 (-20 copies) were added to a suspended bilayer membrane (formed on a silicon substrate with 5 μm holes) reconstituted with Syntaxin/SNAP25 (1:400 protein-to-lipid ratio) \pm Syt7 in the presence of Complexin (2 μM) in solution. The fate of each vesicle before and after the addition of $100 \, \mu$ M Ca²⁺ was monitored by a confocal microscope using a fluorescent (ATTO647N) marker included in the vesicle. **b** Syt7 (included in the t-SNARE containing bilayer) had no impact on the fusion competence of docked Syt1/VAMP2 vesicles, with -85% fusing within 5 s after the arrival of $100 \, \mu$ M Ca²⁺ signal at or near the docked vesicles. The hatched bar represents the percent fusion occurring with 2 frames (-300 ms) following Ca²⁺ arrival. **c** Syt7 altered the Ca²⁺-triggered fusion kinetics of docked Syt1/VAMP2 vesicles. Top, Representative time-lapse image of Ca²⁺-evoked fusion of docked vesicles shows that without Syt7 the vesicles fuse rapidly and synchronously following Ca²⁺

addition. The inclusion of Syt7 (1:200 protein-to-lipid ratio) introduces variable delays in Ca^{2^+} -evoked fusion kinetics. Individual vesicles (white circles) docked within 5 µm suspended bilayer are shown. Bottom, quantitative analysis of Ca^{2^+} -evoked fusion of Syt1/VAMP2 vesicles shows that Syt7 introduces a concentration-dependent delay in the Ca^{2^+} -evoked fusion kinetics, resulting in a significant reduction in the proportion of vesicles fusing within the first 2 frames (-300 ms) following Ca^{2^+} arrival at time t=0 s. Data (mean \pm standard deviation) are from 5 independent experiments (N=5) for each condition (-40–50 vesicles per experiment). One-way ANOVA revealed statistically significant difference (***p<0.001) in Ca^{2^+} -coupled fusion occurring within -300 ms (hatched bar) between groups. The data from ANOVA and Tukey's HSD post-hoc comparing specific groups is shown in Supplementary Table 1. The source data is provided as a 'Source Data' file. Figure 1a created in BioRender. Krishnakumar, S. (2023) BioRender.com/f92r389.

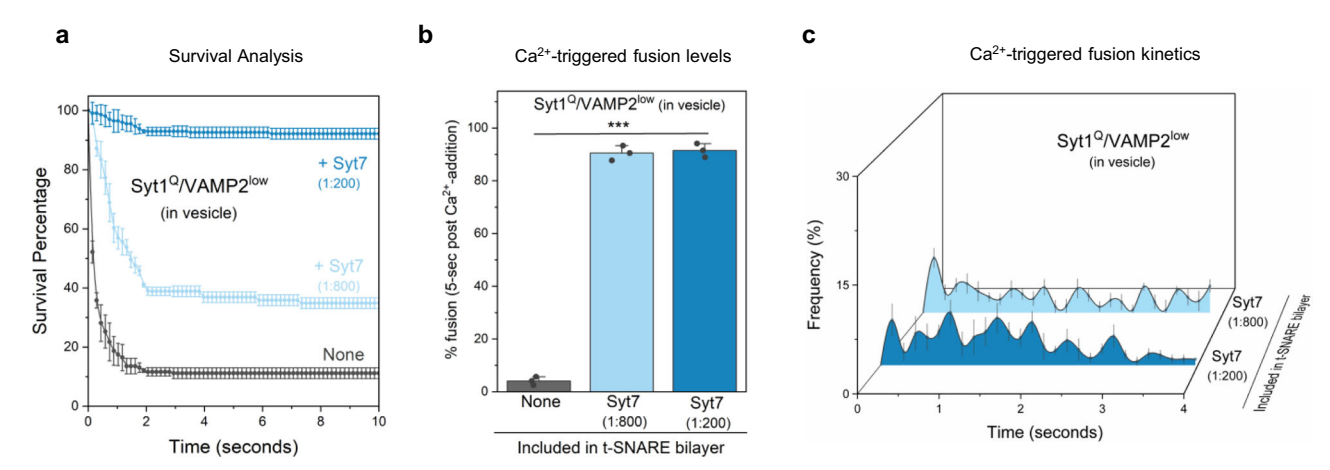


Fig. 2 | **Contribution of Syt7 to the establishment of the fusion clamp.** The involvement of Syt7 in the fusion clamp was evaluated using vesicles containing low-copy VAMP2 (-15 copies) and a non-clamping Syt1 mutant, Syt1^Q (carrying R281A,E295A,Y338W,R398A,R399A mutations that disrupt the Syt1-SNARE primary interface) in the absence of CPX. **a** The time between docking and spontaneous fusion was measured for each docked vesicle and the 'docking-to-fusion' latency time was cumulatively expressed as the survival percentage. This 'survival analysis' provided the measure of the strength of the fusion clamp. In the absence of Syt7 (gray), the majority of the docked VAMP2^{low}/Syt1^Q vesicles proceed to fuse spontaneously with a half-time of -1 s. The inclusion of Syt7 in the bilayer resulted in stably docked vesicles in an immobile state, with clamping efficiency correlating with the amount of Syt7 included. Approximately 40% of vesicles were clamped

under low Syt7 concentration (1:800, light blue) and this increased to -90% under high Syt7 concentration (1:200, dark blue). **b**, **c** Syt7 clamped VAMP2^{low}/Syt1^Q vesicles remained fusion competent and could be triggered to fuse by the addition of Ca²⁺ (100 μ M) and the observed fusion was desynchronized to the Ca²⁺ signal. In the absence of Syt7, a very small percent of the docked VAMP2^{low}/Syt1^Q vesicles underwent fusion which precluded meaningful kinetic analysis. Data (mean \pm standard deviation) are from 3 independent experiments (N = 3) for each condition (-40–50 vesicles per experiment). One-way ANOVA revealed statistically significant difference (***p < 0.001) in % Ca²⁺-evoked fusion of docked vesicles in the presence of Syt7 as compared to the condition without Syt7 in the bilayer. The data from ANOVA and Tukey's HSD post-hoc comparing specific groups are shown in Supplementary Table 2. The source data is provided as a 'Source Data' file.

1:800 and 1:200 Syt7^{WT} respectively) (Fig. 3b). Notably, the observed fusion was desynchronized from the Ca²⁺ signal (Fig. 3b). Taken together, these data suggest that Syt1 and Syt7 act on the same vesicles, likely targeting the same SNARE complexes, and their cooperative action in regulating Ca²⁺-evoked fusion stems from a competitive binding of Syt1 and Syt7 to the same SNARE complex. Furthermore, these results unequivocally demonstrate that Syt1 acts as a 'fast' Ca²⁺-sensor to trigger rapid Ca²⁺-evoked vesicle fusion, whereas Syt7 functions as a 'slow' Ca²⁺-sensor that mediates release over longer time intervals.

Subsequently, we employed a quantitative pull-down assay to directly test the competitive interaction between Syt1 and Syt7 with the same SNARE complex. While the binding of Syt1 to Syntaxin/ SNAP25 is well-documented³⁴⁻³⁶, the Syt7-SNARE interaction remains poorly understood. Hence, we initially conducted a pull-down experiment using Syt7 immobilized on agarose beads as 'bait' and pre-formed CPX-SNARE complex at varying concentrations as the 'prey'. Western-blot analysis confirmed direct molecular interaction between the CPX-SNARE complex and Syt7, revealing a saturable doseresponse curve with an estimated apparent affinity (K_d) ~ 20 µM (Supplementary Fig. 4). We then examined the binding of 30 µM CPX-SNARE complex to Syt7-coated beads in the presence of varying concentrations (ranging from 1 µM to 50 µM) of Syt1. The inclusion of Syt1 disrupted the Syt7-SNARE interaction, resulting in near complete abrogation of binding at Syt1 concentrations $\geq 30 \,\mu\text{M}$ (Fig. 3c). This analysis directly demonstrates the competitive nature of the binding between Syt1 and Syt7 to the SNARE complex. In summary, our data argue that the kinetics of Ca2+-triggered fusion are governed by the number of Syt1 or Syt7 associated SNAREpins, which is in turn determined by the relative abundance of these two proteins.

Differential clamp removal rates of Syt1 and Syt7 shape Ca²⁺ triggered fusion kinetics

How do Syt1 and Syt7 shape the kinetics of vesicular fusion? It has been proposed that the cooperative action of Syt1 and Syt7 in regulating vesicular release can be explained by a 'release of inhibition' model^{10–12}.

According to this model, Syt1 and Syt7 along with CPX bind to SNAREpins at docked SVs and clamp vesicular fusion at rest. Ca²⁺ activation of Syt1 and Syt7 leads to the release of the fusion clamp. Thereby, the rate of the Ca²⁺-triggered removal of the fusion clamp determines the overall efficacy and kinetics of SV fusion (Fig. 4a). The model further posits that the differential Ca²⁺/membrane binding properties of Syt1 and Syt7, along with the relative numbers of Syt1 or Syt7 bound SNAREs on a given vesicle, fine-tune the release properties in response to Ca²⁺ signals. Indeed, our experimental data with Ca²⁺-insensitive Syt1^{DA} and Syt7^{DA} mutants support the 'release of inhibition' model, as both mutants blocked the Ca²⁺-triggered fusion of docked vesicles, consistent with the model predictions (Fig. 3).

To investigate whether the differences in Ca²⁺/membrane binding properties of Syt1 and Syt7 could explain our current results, we adapted the previously developed computational framework¹². This modeling framework enables us to simulate SV fusion in response to specific Ca²⁺ signals for different Synaptotagmin fusion clamp architectures. Drawing on structural studies, within the default model, we assumed that each vesicle contains six SNARE complexes³⁷ and each SNARE complex can bind two Syt1 molecules³⁴. Additionally, we postulated that Syt7 might compete with Syt1 for one of these binding sites. Consequently, we considered two limiting cases for the fusion clamp's architecture: either Syt1/Syt1 or Syt1/Syt7 (Fig. 4a). These scenarios correspond to experimental conditions without Syt7 or with a saturating level of Syt7 in the lipid bilayer respectively. As in our previous work¹², we assumed that Ca²⁺ binding and membrane loop insertion of the C2B domain of Syt1 or C2A domain of Syt7 leads to the instantaneous removal of the fusion clamp (Fig. 4b, Scheme 1). The release of the clamp enables the full zippering of freed SNAREs, and each SNARE complex independently contributes towards lowering the fusion barrier, thereby catalyzing SV fusion.

As a model input, we incorporated experimentally estimated changes in [Ca²⁺] at the lipid bilayer, corresponding to a ramped increase of [Ca²⁺] from 0 to 100 µM (Supplementary Fig. 3). In the absence of Syt7 (Syt1/Syt1 clamp), the standard model closely reproduced the kinetics of vesicular fusion in response to the addition of

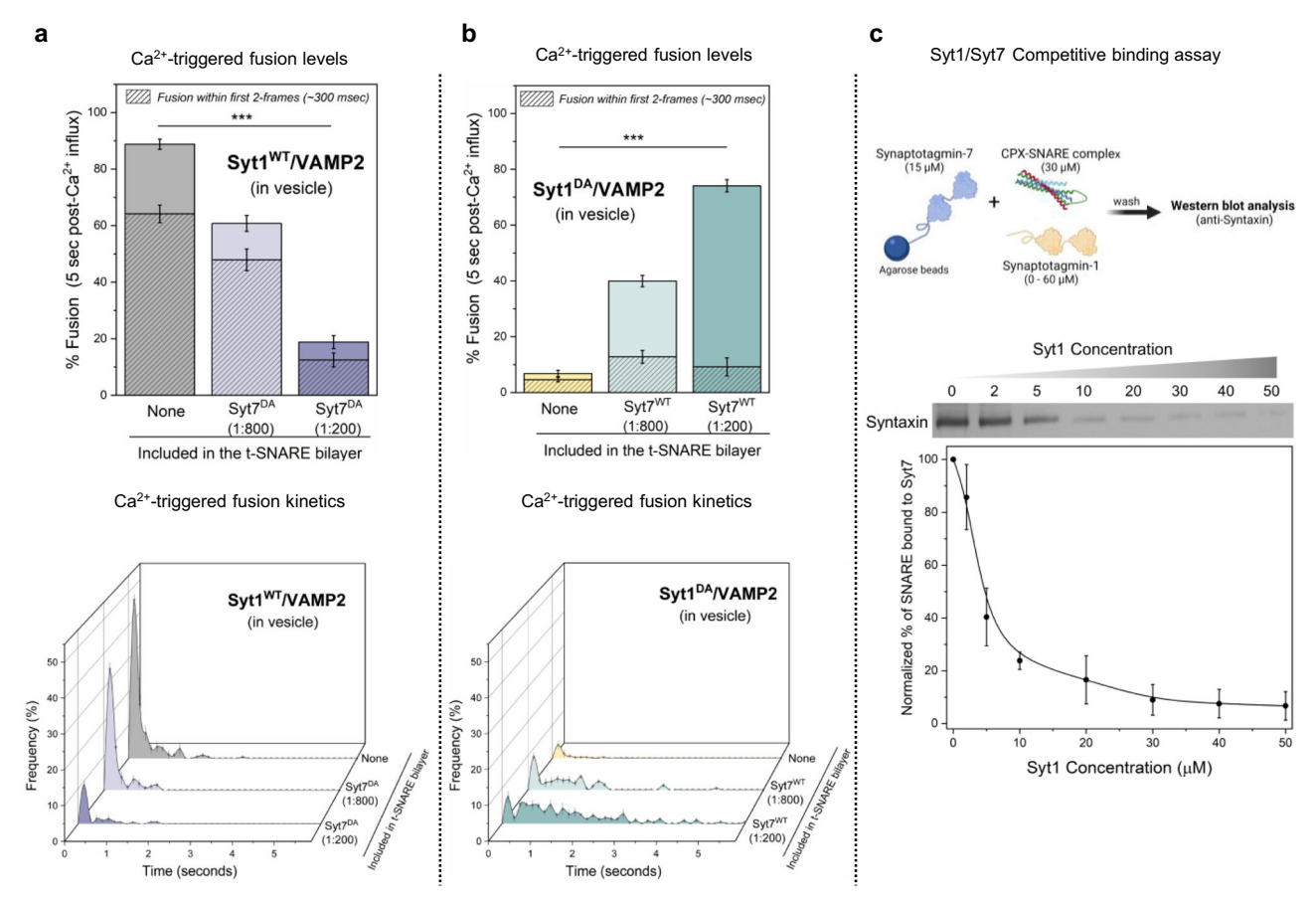


Fig. 3 | **Syt1** and **Syt7** synergistically regulate Ca^{2^+} -evoked fusion via competitive binding to the same SNARE complex. a The inclusion of the Ca^{2^+} binding deficient Syt7 mutant (Syt7^{DA}) in the bilayer inhibited Ca^{2^+} (100 μM) evoked fusion of Syt1^{WT}/ VAMP2 vesicles in a dose-dependent manner, without altering the overall fusion kinetics. **b** Syt7^{WT} from the bilayer rescued the Ca^{2^+} -evoked fusion of Syt1^{DA} /VAMP2 vesicles but the fusion events were desynchronized to the Ca^{2^+} signal. Complexin (2 μM) in solution was included in all experiments. **c** Quantitative pull-down and Western-blot analysis with Syt7 as 'bait' and CPX-SNARE complex as 'prey' demonstrate that Syt1 disrupts Syt7-SNARE interaction in a concentration-

dependent manner. Data (mean \pm standard deviation) are from 5 independent experiments (N=5) for each condition (-40–50 vesicles per experiment) in (\mathbf{a}) and (\mathbf{b}) and from 4 independent experiments (N=4) in (\mathbf{c}). One-way ANOVA revealed statistically significant difference in % Ca^{2^+} -evoked fusion of docked vesicles in the presence of $\mathrm{Syt}^{\mathrm{DA}}$ (***p < 0.001) or $\mathrm{Syt}^{\mathrm{DM}}$ (***p < 0.001) as compared to condition without Syt^7 in the bilayer. The data from ANOVA and Tukey's HSD post-hoc comparing specific groups are shown in Supplementary Tables 3 and 4 respectively. The source data is provided as a 'Source Data' file. Figure 3c (top) created in BioRender. Krishnakumar, S. (2023) BioRender.com/p26b995.

Ca²⁺ (Fig. 4c). Indeed, the time course of Syt1-mediated vesicular fusion closely follows the kinetics of the [Ca²⁺] signal (Fig. 4c). This suggests that Ca²⁺ diffusion is likely the rate-limiting step governing vesicular fusion kinetics under our experimental conditions. However, this model failed to replicate the slower vesicular fusion kinetics observed when Syt7 was included (Syt1/Syt7 clamp).

Under our experimental conditions, Syt1 and Syt7 are predicted to exhibit comparable Ca^{2+} -activation patterns, with Syt7 being slightly more sensitive than Syt1 (Supplementary Fig. 5). This suggests that the Ca^{2+} -triggered membrane insertion of Syt7 is not the rate-limiting step in the removal of the Syt7 fusion clamp. Consequently, we adapted the model to include a delay between the Ca^{2+} -triggered membrane insertion of the Syt7 C2A domain and the removal of the fusion clamp (Fig. 4b, Scheme 2). This modification allowed us to reconcile the model with the experimental data under Syt1/Syt7 clamp conditions (Fig. 4c).

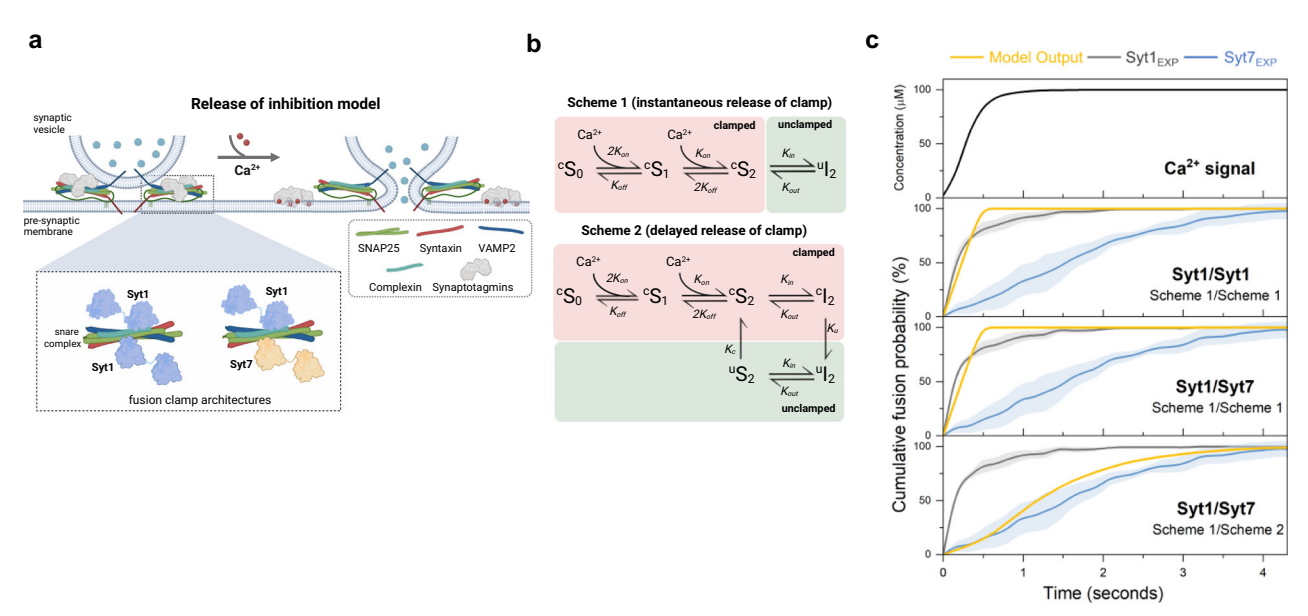
Given the ongoing debate surrounding the exact number of SNARE complexes on an RRP vesicle^{37,38}, as well as the architecture of the Synaptotagmin fusion clamp^{30,34,35}, we explored alternative fusion clamp configurations. Specifically, we varied the number of SNAREpins in the vesicles from six to twelve and examined scenarios where a single Synaptotagmin molecule - either Syt1 or Syt7 - could bind to and clamp an individual SNAREpin (Supplementary Fig. 6). As expected,

increasing the number of SNAREpins, or using a single clamp instead of a dual clamp accelerated fusion rates at low $[Ca^{2+}]$. However, at saturating $[Ca^{2+}]$, the models' outputs closely aligned with those of the default dual-clamp model with six SNAREpins (Supplementary Fig. 6). Taken together, our data argue that the mechanisms of clamp removal are distinct for Syt1 and Syt7 and that the differing rates of clamp removal – rapid for Syt1 and slower for Syt7 – are key factors determining the Ca^{2+} triggered vesicular fusion kinetics.

Syt7 enhances Ca^{2+} synchronized fusion under elevated $[\text{Ca}^{2+}]_{\text{basal}}$ conditions

In addition to modulating fusion kinetics, Syt7 has also been implicated in the facilitation of synchronous neurotransmitter release during neuronal activity^{17,18}. This short-term plasticity of vesicular release has been linked to the accumulation of $[Ca^{2+}]_{residual}$ in low micromolar range within the presynaptic terminal due to sustained neuronal activity^{1,15,16}. Hence, we investigated the effect of elevated basal $[Ca^{2+}]_{basal}$ on Ca^{2+} -triggered release properties of Syt1/VAMP2 vesicles in the absence and presence of Syt7.

The inclusion of $0.5\,\mu\text{M}$ [Ca²⁺]_{basal} during the vesicle docking phase had little to no effect on vesicle docking or clamping (i.e., spontaneous fusion) of vesicles across all conditions tested (Supplementary Fig. 7). It also did not affect vesicle fusion triggered by $100\,\mu\text{M}$



state of the C2 domains, while I_2 refers to membrane inserted state of the Ca^{2^+} -bound C2 domain. The prefixes c and u refer to the 'clamped' or 'unclamped' state respectively. ${\bf c}$ The time course of vesicular fusion (Model Output) simulated in response to the experimentally constrained Ca^{2^+} signal (Supplementary Fig. 3) for models with different clamp architecture and kinetics of clamp reversal. Experimental data (mean \pm standard deviation from Fig. 1c) for the Ca^{2^+} -triggered fusion of Syt1 containing vesicles in the absence (Syt1 $_{\rm EXP}$) or the presence of saturating levels of Syt7 (Syt7 $_{\rm EXP}$) are plotted for comparison. The model suggests that experimentally observed fusion kinetics can be explained by the mechanism with differential rates of fusion clamp removal for Syt1 (instantaneous) and Syt7 (delayed). For each modeled condition a minimum of 1000 stochastic simulations were performed to calculate the average response. The source data is provided as a 'Source Data' file. Figure 4a created in BioRender. Krishnakumar, S. (2023) BioRender.com/x49d271.

[Ca²⁺] under control (no Syt7 in the bilayer) conditions (Fig. 5a). However, when Svt7 was included in the bilayer (at 1:200 protein-tolipid ratio), it enhanced the fast component of Ca²⁺-evoked release (within the first 300 milliseconds after the initial arrival of Ca²⁺ signal), increasing it from ~8% to ~35%, without changing the overall level of fusion over the 5-second interval (Fig. 5a). Likewise, the computational model incorporating a delay in the removal of the Syt7 fusion clamp (Scheme 2) also replicated the synchronization of vesicular fusion when Syt7 was pre-activated with low micromolar [Ca²⁺] (Fig. 5b). We only tested 0.5 μM [Ca²⁺]_{basal} in our in vitro assay as higher [Ca²⁺]_{basal} significantly increased spontaneous fusion of docked vesicles, preventing meaningful analysis. However, the degree of synchronization predicted by the computational model correlated with the concentration of Ca²⁺ utilized for pre-activation (Fig. 5b). Together, these data show that when pre-activated by low micromolar [Ca²⁺]_{basal}, Syt7 enhances Ca2+-synchronized vesicle fusion.

Interestingly, disrupting Ca²⁺-binding to Syt1 (Syt1^{DA}) did not abolish the Syt7-dependent synchronization of vesicular release with elevated [Ca²⁺]_{basal} (Fig. 5a). Indeed, we observed a similar proportion of Ca²⁺-synchronized release between Syt1^{WT}/Syt7 and Syt1^{DA}/Syt7 conditions (Fig. 5a). This indicates that when primed by elevated [Ca²⁺]_{basal}, Syt7 is capable of independently mediating fast Ca²⁺-synchronized release.

Discussion

Our study presents one of the first in vitro reconstitution of different modes of Ca²⁺-triggered SV fusion with minimal protein components. We demonstrate that Syt1 and Syt7, along with SNAREs and CPX, are sufficient to recapitulate fast and delayed Ca²⁺-evoked vesicular fusion

as well as Ca²⁺-dependent facilitation of vesicular release. Our data show that under resting conditions, Svt1, Svt7, CPX work together to arrest SNARE assembly and produce stably, docked RRP-like vesicles. When activated by the Ca²⁺ signal, the Syt1 triggers the fast component, whilst Syt7 drives the slow component of the resultant vesicular fusion. Mutational analysis with Ca2+-insensitive Syt1 and Syt7 mutants indicates that the synergistic action of Syt1 and Syt7 in the regulation of Ca²⁺-evoked vesicular fusion can be described by the 'release of inhibition' model, which posits that the rate of vesicular fusion is governed by the release of the Syt1 and/or Syt7 fusion clamp upon their Ca²⁺ activated membrane insertion^{10–12}. Furthermore, we observe that the kinetics of Syt7-mediated vesicular fusion are significantly influenced by [Ca2+]basal. We demonstrate that Syt7 is capable of mediating fast, Ca2+-synchronized release, independent of Syt1, when [Ca²⁺]_{basal} is elevated into low micromolar range. We posit that this phenomenon underlies the critical role of Syt7 in short-term facilitation of fast synchronous release component during sustained neuronal activity^{1,4}.

The temporal resolution of our fusion assay is limited by the shape of the Ca^{2+} signal, which ramps up to $100~\mu M$ within approximately 750 milliseconds. Indeed, we find that the rate of fast Syt1-mediated fusion closely mirrors the rate of $[Ca^{2+}]$ increase at the lipid bilayer. Due to technical limitations, our in vitro assay cannot replicate the rapid, millisecond-scale Ca^{2+} transients evoked by action potentials at the presynaptic active zone. Hence, we utilized a computational modeling framework, capable of simulating vesicular fusion kinetics in response to specific $[Ca^{2+}]$ transients, to relate our findings to neurotransmitter release kinetics in neuronal synapses. The computational implementation of the 'release of inhibition' model with the experimental

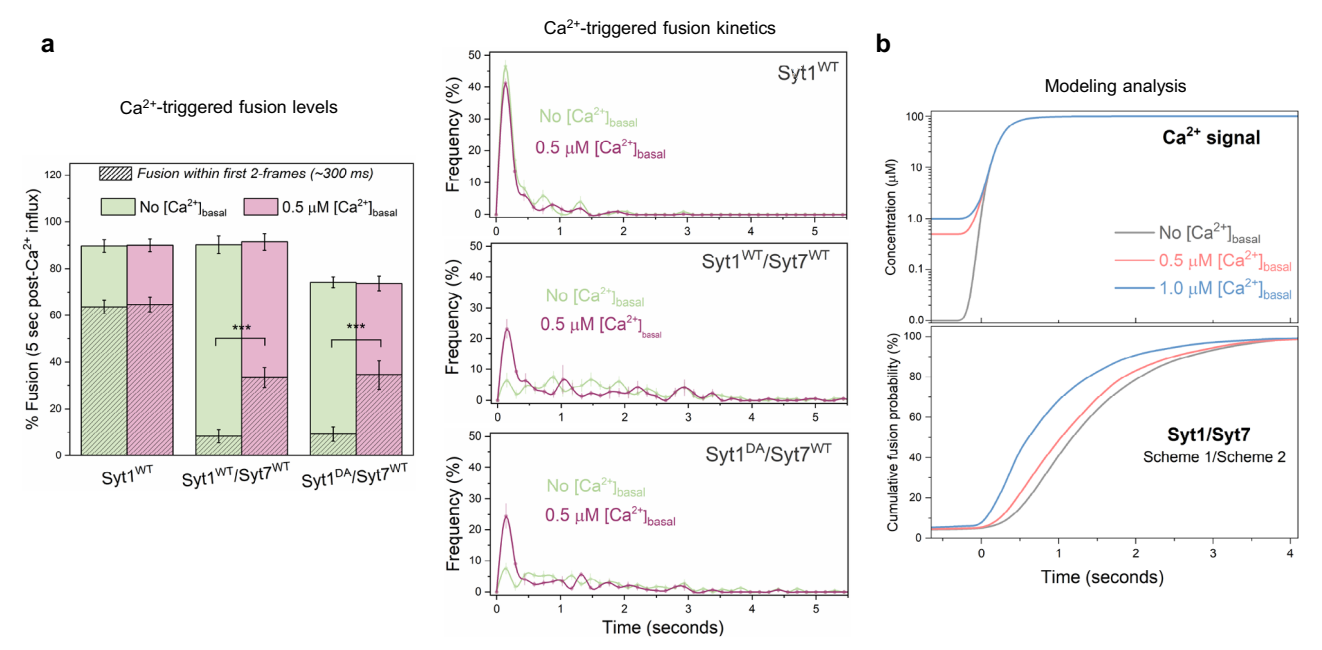


Fig. 5 | **Syt7 enhances Ca²⁺-synchronized fusion under elevated [Ca²⁺]**_{basal} **conditions.** a Comparison of the Ca²⁺ (100 μM) evoked fusion characteristics without (green) or with (pink) 0.5 μM [Ca²⁺]_{basal} included during vesicle docking reveals that when pre-activated, Syt7 (included in the bilayer at 1:200 protein-to-lipid ratio) increases the proportion of Ca²⁺-coupled release of Syt1-containing vesicles (Syt1^{WT}/Syt7^{WT}) without changing the overall fusion levels. This enhancement was not observed with Syt1^{WT} alone. Notably, a similar degree of enhancement of Ca²⁺-synchronized release was observed with vesicles containing Ca²⁺-binding deficient Syt1^{DA} (Syt1^{DA}/Syt7^{WT}). Data (mean \pm standard deviation) are from 5 independent

experiments (N=5) for each condition (-40–50 vesicles per experiment). Complexin ($2\mu M$) in solution was included in all experiments. **b** The dual Syt1/Syt7 clamp model, incorporating the delayed release of the clamp for Syt7, reproduces the experimentally observed enhancement of synchronous release following preactivation with low micromolar [Ca²¹]. The extent of facilitation correlated with the level of pre-activating [Ca²¹] used. For each modeled condition a minimum of 1000 stochastic simulations were performed to compute the average response. ****p < 0.001 using the one-sided students' t-test comparison to the control condition with no [Ca²¹]_{basal}. The source data is provided as a 'Source Data' file.

ramped [Ca²+] signal as an input, closely reproduced the kinetics of Syt1-mediated vesicular fusion observed in our reconstituted fusion assay. Notably, the same model implementation reproduced the millisecond kinetics of vesicular fusion in response to fast [Ca²+] transients observed in live synapses¹². This indicates that the reconstituted fusion assays replicate the functionality of the component proteins in living synapses, with comparable operational efficacy. Thus, our data strongly suggest that Syt1 and Syt7 are likely sufficient to describe the synchronous and asynchronous components of AP-evoked neuro-transmitter release in neuronal synapses.

The computational modeling further suggests that the differential effects of Syt1 and Syt7 on vesicular release kinetics can be attributed to the differential strength and kinetics of Ca2+-triggered reversal of their respective fusion clamps. Specifically, our data indicate that activation leads to almost instantaneous removal of the Syt1 fusion clamp but delayed release of the Syt7 clamp. Both Syt1 and Syt7 are expected to bind and clamp the SNARE complexes via their C2B domains^{34,36}. However, the critical distinction in their roles in the regulation of SV fusion arises from the Ca2+ activation of the Syt1 C2B domain compared to the Syt7 C2A domain¹⁹. The fast removal of the Syt1 clamp may be attributed to the rapid dissociation of Syt1 from the SNARE complex at the primary interface upon Ca2+-triggered membrane insertion of its C2B domain, as demonstrated in biochemical and structural studies^{35,36}. In contrast, for Syt7 the decoupling of SNARE binding (C2B domain) and Ca2+ activation (C2A domain) may contribute to the slower disassembly of the Syt7 fusion clamp.

While our data indicates that Syt1, Syt7, and CPX all are involved in establishing the fusion clamp, the precise molecular composition of the fusion clamp on a RRP vesicle remains unknown. In particular, the clamping function of CPX and Syt7 remains a topic of debate. For example, genetic removal of CPX potentiates spontaneous events in invertebrate model systems^{39,40}, but acute removal of CPX in cultured

mouse neurons abates both spontaneous and evoked neurotransmitter release⁴¹ suggesting that CPX is principally a positive regulator of fusion in mammalian synapses. However, a recent study showed that CPX mutants that disrupt the clamping function under in vitro conditions^{26,42} selectively potentiate spontaneous neurotransmitter release, while leaving the evoked release largely untouched⁴². This suggests that the inhibitory function of CPX might be normally masked by a more pronounced positive function in mammalian synapses. Similarly, in central synapses the genetic deletion of Syt7 does not alter frequency of spontaneous release¹⁹. However, the overexpression of Syt7 reverses the increased mini frequency observed in Syt1 knockout neurons¹⁹. This suggests that Syt7 can substitute for Syt1 in clamping mini release, but its clamping role may not be apparent under normal physiological conditions due to low expression levels of Syt7 in presynaptic terminals. Additional research is needed to delineate the precise molecular organization of the prefusion 'clamped' state and the mechanisms of Ca²⁺-triggered reversal of the fusion clamp.

Additionally, we find that Syt1 and Syt7 compete to bind the same SNARE complexes. Consequently, the relative abundance of these Ca^{2+} sensors shape the kinetics and plasticity of Ca^{2+} -evoked vesicular fusion in our assay. This observation offers a mechanistic explanation for physiological data demonstrating that the relative expression levels of Syt1 and Syt7 regulate both the kinetics and plasticity of neurotransmitter release in neuronal synapses^{43,44}. The number of Syt1 per vesicle is tightly controlled (-15–20 copies per SV) and local Syt1 concentration under a docked vesicle is estimated to be in the range of 5–10 mM^{45,46}. Syt1 interacts with SNARE complex at the primary interface with an affinity of -10 μ M, suggesting a near-complete saturation of Syt1-SNARE binding under physiological conditions. However, the precise concentration of Syt7 is unknown and varies across synapses. Consequently, the number of Syt1- or Syt7-bound SNAREpins under a

given RRP vesicle is likely determined by local abundance of Syt7. This implies that controlling the local abundance of Syt7 molecules could be a straightforward mechanism by which synapses can dynamically adjust the strength and efficacy of synaptic transmission during sustained activity.

While the precise mechanism of Svt7-mediated facilitation is not fully understood, it is hypothesized that activation of Syt7 could enhance the release by two different mechanisms: (i) by increasing the probability of RRP vesicles and/or (ii) by enhancing the activitydependent docking of SVs^{4,47}. Our in vitro reconstitution experiments and modeling demonstrate that, when pre-activated, Syt7 enhances the synchronous release of pre-docked vesicles. Our previous computational modeling study provided insights into the possible molecular mechanisms underlying Syt7-mediated facilitation¹². It revealed that the rate of vesicle fusion is dictated by the time taken for three SNAREpins to be released from the fusion clamp on a specific vesicle. Due to its high Ca²⁺/membrane affinity, Syt7 is partially activated at low micromolar [Ca²⁺], weakening the fusion clamp. This in turn, accelerates the liberation of three SNAREpins upon the arrival of [Ca²⁺] signal, thereby enhancing the fast release component. Consistent with this hypothesis, we observed a comparable level of facilitation when [Ca²⁺]_{basal} levels were elevated either during or after the vesicles reached the immobile clamped state (Supplementary Fig. 7).

We note that, apart from the distinct Ca2+-release sensors, other proteins and mechanisms also play a role in regulating the timing and plasticity of neurotransmitter release. For example, the genetic deletion of Syt7 does not fully eliminate asynchronous release or shortterm facilitation in some synapses^{43,48}. Consequently, it is suggested that other Ca²⁺-release sensors (e.g., Syt1, Syt3 and Doc2A) may also contribute to the asynchronous release component^{21-23,49}. Additionally, short-term facilitation of synchronous neurotransmitter release may result from enhanced Ca2+ transients at release sites, driven by the saturation of Ca²⁺ buffers during repetitive activity^{25,50}. Furthermore, the strength and efficacy of neurotransmitter release is also regulated by Ca²⁺-dependent SV docking, priming, and recycling. As such, SV priming factors (e.g. RIM, Munc13) could also influence neurotransmitter release dynamics^{9,51}. Nonetheless, our results highlight the central role of Syt1 and Syt7 in decoding presynaptic Ca2+ dynamics and translating this into complex patterns of vesicular release.

Methods

Proteins & materials

In this study, we used the following clones that have been described previously^{26,30} including full-length VAMP2 (human VAMP2-His⁶, residues 1–116); full-length t-SNARE complex (mouse His⁶-SNAP25B, residues 1–206 and rat Syntaxin1A, residues 1–288); CPX (human His⁶-Complexin 1, residues 1–134); Syt1 wild-type (rat Synaptotagmin1-His⁶, residues 57-421) and mutants (D309A, D 363A, D365A; Syt1^{DA}) and (R281A, E295A, Y338W, R398A, R399A, Syt1^Q) in the same background.

Our initial experiments were conducted with the full-length Syt7 wild-type protein (His⁶-SUMO-rat Synaptotagmin-7, residues 17–403). However, this construct posed technical challenges due to its low and highly variable membrane reconstitution efficiency. Hence, we modified the construct by adding a second transmembrane domain (TMD) from Syt1 with a flexible 16 residue GSGS linker, resulting in His⁶-SUMO-Syt1^{TMD}-Syt7 construct (referred to as Syt7^{WT} in this manuscript). The inclusion of Syt1^{TMD} (in addition to the Syt7^{TMD}) improved the reconstitution efficiency of the Syt7^{WT} protein into the membrane, while the flexible GSGS linker ensured the proper orientation of the two TMDs and Syt7 C2AB domains (Supplementary Fig. 1). Control experiments showed that effect of Syt7, whether containing one or two TMDs, on Ca²⁺-evoked fusion of Syt1/VAMP2 vesicles were indistinguishable (Supplementary Fig. 1).

We also generated Syt7 mutant (D225A, D227A, D233A, D357A, D359A; Syt7^{DA}) in the same background. We purchased the cDNA to

produce the SUMO nanobody (nanoCLAMP SMT3-A1) from Nectagen (Lawrence, KS). The lipids used in the study, including 1,2-dioleoyl -snglvcero-3-phosphocholine (DOPC). 1.2-dioleovl-sn-glycero-3-(phospho-L-serine) (DOPS), and phosphatidylinositol 5-bisphosphate (PIP2) were purchased from Avanti Polar Lipids (Alabaster, AL), ATTO647N-DOPE and ATTO465-DOPE were purchased from ATTO-TEC, GmbH (Siegen, Germany) and Calcium Green conjugated to a lipophilic 24-carbon alkyl chain (Calcium Green C24) was purchased from Abcam (Cambridge, UK). All other research materials and consumables, unless specified, were purchased from Sigma-Aldrich (St Louis, MO) and Thermo Fisher Scientific (Waltham, MA)

Protein expression and purification

All proteins were expressed and purified in a bacterial expression system as described previously^{26,30} (Supplementary Fig. 1). In summary, proteins were expressed in E. coli BL21(DE3) cells (Novagen, Madison, WI) under 0.5 mM IPTG induction for 4 h. Bacterial cells were pelleted and then lysed using a cell disruptor (Avestin, Ottawa, Canada) in lysis buffer containing 25 mM HEPES, 400 mM KCl, 4% Triton X-100, 10% glycerol, pH 7.4 with 0.2 mM Tris[2-carboxyethyl] phosphinehydrochloride (TCEP), and EDTA-free Complete protease inhibitor cocktail (Merck, Rahway, NJ). The resulting lysate was clarified using a 45Ti rotor (Beckman Coulter, Atlanta, GA) at 40,000 RPM for 30 min and subsequently incubated with pre-equilibrated Ni-NTA resin overnight at 4 °C. The resin was washed with wash buffer containing 25 mM HEPES pH 7.4, 400 mM KCl, 0.2 mM TCEP. The wash buffer was supplemented with 1% octylglucoside (OG) for Syt1 and SNARE, and with 0.2% Triton-X-100 for Syt7. Proteins were eluted from beads using 400 mM Imidazole and their concentrations were determined using a Bradford Assay (BioRad, Hercules, CA) with BSA standard. The Syt1 and Syt7 proteins were further treated with Benzonase (Millipore Sigma, Burlington, MA) at room temperature for 1h with Syt1 additionally being run through ion exchange (Mono S) to remove DNA/RNA contamination. SDS-PAGE analysis was done to check the purity of the proteins, and all proteins were flash-frozen in small aliquots and stored at -80 °C with 10% glycerol.

Vesicle preparation

Small unilamellar vesicles containing VAMP2 and Syt1 were prepared using rapid detergent dilution and dialysis method, followed by additional purification on discontinuous Optiprep gradient by ultracentrifugation^{26,30}. To mimic synaptic vesicle lipid composition, we used 88% DOPC, 10% DOPS, and 2% ATTO647N-PE, with the protein-to-lipid input ratio of 1:100 for VAMP2 for physiological density, 1:500 for VAMP2 at low copy number, and 1:250 for Syt1. Informed by previous work^{26,30} that characterized the reconstitution efficiency and inside/outside ratio of these proteins, we estimate the vesicle contains -70 copies of outside facing VAMP2 and -20 copies of outside facing Syt1 (at physiological conditions) and -15 copies of VAMP2 and -20 copies of Syt1 (under low VAMP2 conditions).

Suspended lipid bilayer formation

To form the suspended lipid bilayer, we first prepared giant unilamellar vesicles (GUVs) containing t-SNARE ± Syt7 were prepared using the osmotic shock protocol as described previously⁵². To mimic the presynaptic plasma membrane, the lipid composition of the GUVs was 80% DOPC, 15% DOPS, 3% PIP2%, and 2% ATTO465-PE. The t-SNARE complex (1:1 Syntaxin/SNAP25) was included at the protein-to-lipid input ratio of 1:200 to yield a final concentration of 1:400. Incorporating the t-SNARE complex enabled us to circumvent the necessity for the SNARE-assembling chaperones Munc18 and Munc13⁵³. When warranted, Syt7 was added at a protein-to-lipid input ratio of 1:50, 1:100, 1:200, and 1:1000 to yield the defined concentrations of Syt7 tested, based on the reconstitution efficiency (-50%) and 50-50 inside/outside

ratio determined by protease (Chymotrypsin) accessibility assay (Supplementary Fig. 1).

Subsequently, t-SNARE (\pm Syt7) containing GUVs were burst on freshly plasma-cleaned Si/SiO₂ chips decorated with a regular array of 5 μ m diameter holes in HEPES buffer (25 mM HEPES, 125 mM KCl, 0.2 mM TCEP, 5 mM MgCl₂ pH 7.4). The bilayers were then extensively washed with the same HEPES buffer containing 1 mM MgCl₂. For each experiment, the fluidity of the bilayers was verified using FRAP of the Atto-465 fluorescence (Supplementary Fig. 8). As a control, we tested and confirmed that the mobility of Alexa488 labeled t-SNAREs is not affected by the inclusion of Syt7 (Supplementary Fig. 8).

Single vesicle fusion assays

The vesicle docking and fusion experiments were carried out as described previously^{26,28,30}. Typically, in each experiment, approximately 100 nM lipids worth of vesicles, along with CPX (2 µM final concentration) were added using a pipette and then allowed to interact with the suspended bilayer for 5 mins. ATTO647N-PE fluorescence was used to track the fate of individual vesicles, i.e. vesicle docking, postdocking diffusion, docking-to-fusion delays, and spontaneous fusion events. Docked immobile vesicles that remained un-fused during the initial 10 min observation period were defined as 'clamped'. Fusion was identified as a sharp, rapid decrease in fluorescence intensity, as the lipids from the vesicles diffused into the bilayer. After the initial 5-minute observation period, the excess vesicles in the chamber were removed by buffer exchange, and 100 µM CaCl₂ was added to quantify the Ca²⁺-triggered fusion of the pre-docked vesicles. To cover large areas of the planar bilayer and simultaneously record lipid mixing in large ensembles of vesicles (-40-50 per experiment), the movies were acquired at a speed of 147 ms per frame.

 Ca^{2^+} typically reached the vicinity of vesicles docked on the bilayer approximately 1-2 frames post-addition 26,30 and this correlated with the minima of the transmittance signal (Supplementary Fig. 3). For select experiments, we also included Calcium Green C24 in the bilayer to directly quantify the arrival of Ca^{2^+} at the bilayer and confirmed that it matched with the transmittance signal change (Supplementary Fig. 3). As Calcium-green is a high-affinity Ca^{2^+} sensor (K_d of -100 nM), its fluorescence signal is typically saturated within a single frame following the arrival of Ca^{2^+} at the bilayer (Supplementary Fig. 3). Hence, we utilized a soluble Alexa647 dye (-25 nM) mixed with 100 μ M $CaCl_2$ to track the diffusion of Ca^{2^+} into the chamber. Assuming similar diffusion of Ca^{2^+} and the Alexa647 dye, the changes in Alexa647 fluorescence provided a reliable indicator for estimating alterations in the $[Ca^{2^+}]$ signal at or near the vesicles docked on the bilayer (Supplementary Fig. 3).

All experiments were carried out at 37 $^{\circ}$ C using an inverted laser scanning confocal microscope (Leica-SP5) equipped with a multi-wavelength argon laser including 488 nm, diode lasers (532 nm and 641 nm), and a long-working distance 40X water immersion objective (NA 1.1). The emission light was spectrally separated and collected by photomultiplier tubes.

Pull-down binding analysis

To investigate the binding of Syt7 to SNAREs and assess the competitive binding of Syt1/Syt7 to the same SNARE complex, we used a pull-down analysis coupled with western-blot analysis. Briefly, we purified a SUMO-nanobody and covalently attached it to a CNBR-activated Sepharose resin. The nanobody-Sepharose resin was incubated (4 hr at 4 °C) with SUMO-Syt7 protein and subjected to extensive wash with HEPES buffer (50 mM HEPES, 400 mM KCl, 0.2 mM TCEP, 0.2% Triton-X-100, pH 7.4) to form the 'bait'. The CPX-SNARE complex was assembled and purified on the Superdex-200 column as described previously 54,55 in the HEPES buffer and used as the 'prey'. For the binding experiment, -15 μ M of Syt7-resin was incubated with pre-formed CPX-SNARE complex at varying (1–50 μ M)

concentrations overnight at 4 °C with minimum agitation. The resin was washed extensively (5X) with HEPES buffer, followed by a stringent wash with HEPES buffer containing 1M KCl to eliminate unbound proteins. The resin samples were subjected to SDS-PAGE gel electrophoresis, followed by western blotting using a Syntaxin monoclonal antibody (Abcam, Cambridge, UK) to quantify the amount of SNARE bound to the Syt7-resin. We used the same protocol for the competition assay, with the following modification: $15\,\mu\text{M}$ Syt7-resin was incubated with $30\,\mu\text{M}$ of CPX-SNARE complex, along with $1\text{--}60\,\mu\text{M}$ Syt1 included in the solution overnight at $4\,^{\circ}\text{C}$ with minimum agitation.

Computational modeling

Vesicular fusion in response to experimentally estimated changes in [Ca²⁺] was simulated using the computational modeling framework established in our previous work¹². [Ca²⁺] stimulation profile was approximated based on the diffusion kinetics of Alexa 647 (Supplementary Fig. 3). Each RRP vesicle was associated with either six or twelve partially assembled SNAREpins which were clamped in this state by either one (Svt1 or Svt7) or two Synaptotagmins (Svt1/Svt1 or Svt1/ Syt7). The dynamics of each Synaptotagmin C2 domain were described by the Markov kinetic schemes shown in Fig. 4b using the parameters we previously constrained. We assumed that k_{on} was limited by diffusion to $1 \,\mu\text{M}^{-1}\,\text{ms}^{-1}$ and $k_{off} = 150\,\,\text{ms}^{-1}$ based on the intrinsic Ca²⁺ affinity $K_d = 150 \,\mu\text{M}$, which is similar for both Syt1 and Syt7 C2 domains^{20,56,57}. $k_{in} = 100 \text{ ms}^{-1}$ based on the characteristic time for Synaptotagmin C2 domain rotation and membrane insertion⁴⁵. $k_{out} = 0.67 \text{ ms}^{-1}$ for Syt1 and $k_{out} = 0.02 \text{ ms}^{-1}$ for Syt7 were determined from the apparent rates of C2 domain dissociation from lipid membranes (k_{diss}) measured in the presence of EGTA using stopped-flow experiments^{57–59} as described in our previous work¹². In reaction Scheme 1 (Fig. 4b), we considered that C2 domain membrane insertion leads to the instantaneous release of the fusion clamp. In reaction Scheme 2 (Fig. 4b), we assumed that a delay between the Ca²⁺-triggered membrane insertion of the Svt7 C2A domain and the removal of the fusion clamp is described by a first-order reaction with the rate $k_{\mu} = 0.0002 \,\mathrm{ms^{-1}}$ (this value was chosen as it best fits the experimental data within the tested k_u range of 0.0001–0.01 ms⁻¹). We further assumed that the clamp could be restored following membrane dissociation at an identical rate $k_c = 0.0002 \,\mathrm{ms^{-1}}$. The rate of vesicular fusion was determined by assuming that the repulsive forces between a docked vesicle and the plasma membrane amount to an energy barrier $E_0 = 26 \text{ k}_B \text{T}^{60}$. Once both of its Synaptotagmins are in an unclamped state a SNAREpin contributes $\Delta E = 4.5 \text{ k}_B \text{T}$ of work towards overcoming this energy barrier 61 . With n uninhibited SNAREpins the fusion barrier is spontaneously overcome through thermal fluctuations at a rate given by the Arrhenius equation $R_{rate}(n) = A \cdot \exp(-\frac{E_0 - n\Delta E}{k_B T})$, where the pre-factor $A = 2.17 \times 10^9 \, \mathrm{s}^{-1}$ considering that a single SNARE complex can mediate fusion in vitro on a timescale of 1 sec^{45,61}. Monte Carlo estimates of the cumulative probability of vesicle fusion in response to a Ca²⁺ activation signal were derived from at least 1000 stochastic simulations of individual vesicles in all scenarios. We estimate that this restricts prediction error due to stochastic variation to less than 1%. All simulations were carried out in MATLAB 2020b (The MathWorks Inc.) and Python 3.10. To accommodate the observed variability in the timing of Ca²⁺ signal arrival, which can span up to three frames under our experimental conditions (see Supplementary Fig. 3), we applied a temporal blurring of the model output, by smoothing the data across a time window of 0.45 s, equivalent to the duration of three imaging frames.

Reporting summary

Further information on research design is available in the Nature Portfolio Reporting Summary linked to this article.

Data availability

All relevant data that support the findings of this study has been included in the 'Source Data' file. Additional supporting information is available from the corresponding author upon request. Source data are provided with this paper.

Code availability

The MATLAB and Python codes used in this study has been deposited in the GitHub repository: (https://github.com/ChrisAlexNorman/SytSim Matlab); (https://github.com/ChrisAlexNorman/SytSim).

References

- Kaeser, P. S. & Regehr, W. G. Molecular mechanisms for synchronous, asynchronous, and spontaneous neurotransmitter release. *Annu Rev. Physiol.* 76, 333–363 (2014).
- Sudhof, T. C. Neurotransmitter release: the last millisecond in the life of a synaptic vesicle. Neuron 80, 675–690 (2013).
- Regehr, W. G. Short-term presynaptic plasticity. Cold Spring Harb. Perspect. Biol. 4, a005702 (2012).
- Jackman, S. L. & Regehr, W. G. The Mechanisms and Functions of Synaptic Facilitation. *Neuron* 94, 447–464 (2017).
- Reyes, A. et al. Target-cell-specific facilitation and depression in neocortical circuits. Nat. Neurosci. 1, 279–285 (1998).
- Abbott, L. F. & Regehr, W. G. Synaptic computation. *Nature* 431, 796–803 (2004).
- 7. Mendonca, P. R. F. et al. Asynchronous glutamate release is enhanced in low release efficacy synapses and dispersed across the active zone. *Nat. Commun.* **13**, 3497 (2022).
- Sudhof, T. C. & Rothman, J. E. Membrane fusion: grappling with SNARE and SM proteins. Science 323, 474–477 (2009).
- Kaeser, P. S. & Regehr, W. G. The readily releasable pool of synaptic vesicles. Curr. Opin. Neurobiol. 43, 63–70 (2017).
- Volynski, K. E. & Krishnakumar, S. S. Synergistic control of neurotransmitter release by different members of the synaptotagmin family. Curr. Opin. Neurobiol. 51, 154–162 (2018).
- Brunger, A. T., Leitz, J., Zhou, Q., Choi, U. B. & Lai, Y. Ca2+-Triggered Synaptic Vesicle Fusion Initiated by Release of Inhibition. *Trends Cell Biol.* 28, 631–645 (2018).
- Norman, C. A., Krishnakumar, S. S., Timofeeva, Y. & Volynski, K. E. The release of inhibition model reproduces kinetics and plasticity of neurotransmitter release in central synapses. Commun. Biol. 6, 1091 (2023).
- Geppert, M. et al. Synaptotagmin I: a major Ca2+ sensor for transmitter release at a central synapse. Cell 79, 717–727 (1994).
- Xu, J., Mashimo, T. & Sudhof, T. C. Synaptotagmin-1, -2, and -9: Ca(2+) sensors for fast release that specify distinct presynaptic properties in subsets of neurons. *Neuron* 54, 567-581 (2007).
- Atluri, P. P. & Regehr, W. G. Delayed release of neurotransmitter from cerebellar granule cells. J. Neurosci. 18, 8214–8227 (1998).
- Hefft, S. & Jonas, P. Asynchronous GABA release generates longlasting inhibition at a hippocampal interneuron-principal neuron synapse. *Nat. Neurosci.* 8, 1319–1328 (2005).
- Huson, V. & Regehr, W. G. Diverse roles of Synaptotagmin-7 in regulating vesicle fusion. *Curr. Opin. Neurobiol.* 63, 42–52 (2020).
- Jackman, S. L., Turecek, J., Belinsky, J. E. & Regehr, W. G. The calcium sensor synaptotagmin 7 is required for synaptic facilitation. Nature 529, 88–91 (2016).
- Bacaj, T. et al. Synaptotagmin-1 and synaptotagmin-7 trigger synchronous and asynchronous phases of neurotransmitter release. Neuron 80, 947–959 (2013).
- Voleti, R., Tomchick, D. R., Sudhof, T. C. & Rizo, J. Exceptionally tight membrane-binding may explain the key role of the synaptotagmin-7 C2A domain in asynchronous neurotransmitter release. *Proc. Natl Acad. Sci. USA* 114, E8518–E8527 (2017).

- Wu, Z. et al. Synaptotagmin 7 docks synaptic vesicles to support facilitation and Doc2alpha-triggered asynchronous release. *Elife* 12, https://doi.org/10.7554/eLife.90632 (2024).
- Yao, J., Gaffaney, J. D., Kwon, S. E. & Chapman, E. R. Doc2 is a Ca2+ sensor required for asynchronous neurotransmitter release. *Cell* 147, 666–677 (2011).
- Weingarten, D. J. et al. Synaptotagmins 3 and 7 mediate the majority of asynchronous release from synapses in the cerebellum and hippocampus. Cell Rep. 43, 114595 (2024).
- 24. Eggermann, E., Bucurenciu, I., Goswami, S. P. & Jonas, P. Nanodomain coupling between Ca(2)(+) channels and sensors of exocytosis at fast mammalian synapses. *Nat. Rev. Neurosci.* **13**, 7–21 (2011).
- Timofeeva, Y. & Volynski, K. E. Calmodulin as a major calcium buffer shaping vesicular release and short-term synaptic plasticity: facilitation through buffer dislocation. Front. Cell Neurosci. 9, 239 (2015).
- Bera, M., Ramakrishnan, S., Coleman, J., Krishnakumar, S. S. & Rothman, J. E. Molecular Determinants of Complexin Clamping and Activation Function. *Elife* 11, e71938 (2022).
- 27. Ramakrishnan, S. et al. Synaptotagmin oligomers are necessary and can be sufficient to form a Ca(2+) -sensitive fusion clamp. *FEBS Lett.* **593**, 154–162 (2019).
- Ramakrishnan, S. et al. High-Throughput Monitoring of Single Vesicle Fusion Using Freestanding Membranes and Automated Analysis. *Langmuir* 34, 5849–5859 (2018).
- Kalyana Sundaram, R. V. et al. Roles for diacylglycerol in synaptic vesicle priming and release revealed by complete reconstitution of core protein machinery. Proc. Natl Acad. Sci. USA 120, e2309516120 (2023).
- Ramakrishnan, S., Bera, M., Coleman, J., Rothman, J. E. & Krishnakumar, S. S. Synergistic roles of Synaptotagmin-1 and complexin in calcium-regulated neuronal exocytosis. *Elife* 9, https://doi.org/10. 7554/eLife.54506 (2020).
- Vevea, J. D. et al. Synaptotagmin 7 is targeted to the axonal plasma membrane through gamma-secretase processing to promote synaptic vesicle docking in mouse hippocampal neurons. *Elife* 10, e67261 (2021).
- 32. Sugita, S. et al. Synaptotagmin VII as a plasma membrane Ca(2+) sensor in exocytosis. *Neuron* **30**, 459–473 (2001).
- 33. Zhou, Q. et al. Architecture of the synaptotagmin-SNARE machinery for neuronal exocytosis. *Nature* **525**, 62–67 (2015).
- Zhou, Q. et al. The primed SNARE-complexin-synaptotagmin complex for neuronal exocytosis. Nature 548, 420–425 (2017).
- Voleti, R., Jaczynska, K. & Rizo, J. Ca(2+)-dependent release of synaptotagmin-1 from the SNARE complex on phosphatidylinositol 4,5-bisphosphate-containing membranes. *Elife* 9, https://doi.org/ 10.7554/eLife.57154 (2020).
- 36. Grushin, K. et al. Structural basis for the clamping and Ca(2+) activation of SNARE-mediated fusion by synaptotagmin. *Nat. Commun.* **10**, 2413 (2019).
- Radhakrishnan, A. et al. Symmetrical arrangement of proteins under release-ready vesicles in presynaptic terminals. Proc. Natl Acad. Sci. USA 118, https://doi.org/10.1073/pnas.2024029118 (2021).
- 38. Bera, M. et al. Synaptophysin chaperones the assembly of 12 SNAREpins under each ready-release vesicle. *Proc. Natl Acad. Sci. USA* **120**, e2311484120 (2023).
- Huntwork, S. & Littleton, J. T. A complexin fusion clamp regulates spontaneous neurotransmitter release and synaptic growth. *Nat. Neurosci.* 10, 1235–1237 (2007).
- 40. Martin, J. A., Hu, Z., Fenz, K. M., Fernandez, J. & Dittman, J. S. Complexin has opposite effects on two modes of synaptic vesicle fusion. *Curr. Biol.* **21**, 97–105 (2011).
- Lopez-Murcia, F. J., Reim, K., Jahn, O., Taschenberger, H. & Brose, N. Acute Complexin Knockout Abates Spontaneous and Evoked Transmitter Release. Cell Rep. 26, 2521–2530.e2525 (2019).

- Malsam, J. et al. Complexin Suppresses Spontaneous Exocytosis by Capturing the Membrane-Proximal Regions of VAMP2 and SNAP25. Cell Rep. 32, 107926 (2020).
- Turecek, J. & Regehr, W. G. Neuronal Regulation of Fast Synaptotagmin Isoforms Controls the Relative Contributions of Synchronous and Asynchronous Release. *Neuron* 101, 938–949.e934 (2019).
- Weyrer, C., Turecek, J., Harrison, B. & Regehr, W. G. Introduction of synaptotagmin 7 promotes facilitation at the climbing fiber to Purkinje cell synapse. *Cell Rep.* 36, 109719 (2021).
- Rothman, J. E., Krishnakumar, S. S., Grushin, K. & Pincet, F. Hypothesis - buttressed rings assemble, clamp, and release SNAREpins for synaptic transmission. FEBS Lett. 591, 3459–3480 (2017).
- 46. Tagliatti, E. et al. Synaptotagmin oligomers clamp and regulate different modes of neurotransmitter release. *Proc. Natl Acad. Sci. USA*, https://doi.org/10.1073/pnas.1920403117 (2020).
- Wu, Z. K., et al. Synaptotagmin 7 docks synaptic vesicles to support facilitation and Doc2α-triggered asynchronous release. *Elife* 12, RP90632 (2023).
- 48. Luo, F. & Sudhof, T. C. Synaptotagmin-7-Mediated Asynchronous Release Boosts High-Fidelity Synchronous Transmission at a Central Synapse. *Neuron* **94**, 826–839.e823 (2017).
- 49. Xue, R., Gaffaney, J. D. & Chapman, E. R. Structural elements that underlie Doc2beta function during asynchronous synaptic transmission. *Proc. Natl Acad. Sci. USA* **112**, E4316–E4325 (2015).
- Matveev, V., Zucker, R. S. & Sherman, A. Facilitation through buffer saturation: constraints on endogenous buffering properties. *Bio*phys. J. 86, 2691–2709 (2004).
- Korber, C. & Kuner, T. Molecular Machines Regulating the Release Probability of Synaptic Vesicles at the Active Zone. Front Synaptic Neurosci. 8, 5 (2016).
- 52. Motta, I. et al. Formation of Giant Unilamellar Proteo-Liposomes by Osmotic Shock. *Langmuir* **31**, 7091–7099 (2015).
- Baker, R. W. & Hughson, F. M. Chaperoning SNARE assembly and disassembly. Nat. Rev. Mol. Cell Biol. 17, 465–479 (2016).
- 54. Krishnakumar, S. S. et al. A conformational switch in complexin is required for synaptotagmin to trigger synaptic fusion. *Nat. Struct. Mol. Biol.* **18**, 934–940 (2011).
- 55. Kummel, D. et al. Complexin cross-links prefusion SNAREs into a zigzag array. *Nat. Struct. Mol. Biol.* **18**, 927–933 (2011).
- Radhakrishnan, A., Stein, A., Jahn, R. & Fasshauer, D. The Ca2+ affinity of synaptotagmin 1 is markedly increased by a specific interaction of its C2B domain with phosphatidylinositol 4,5bisphosphate. J. Biol. Chem. 284, 25749–25760 (2009).
- 57. Davis, A. F. et al. Kinetics of synaptotagmin responses to Ca2+ and assembly with the core SNARE complex onto membranes. *Neuron* **24**, 363–376 (1999).
- Hui, E. et al. Three distinct kinetic groupings of the synaptotagmin family: candidate sensors for rapid and delayed exocytosis. Proc. Natl Acad. Sci. USA 102, 5210–5214 (2005).
- 59. Brandt, D. S., Coffman, M. D., Falke, J. J. & Knight, J. D. Hydrophobic contributions to the membrane docking of synaptotagmin 7 C2A domain: mechanistic contrast between isoforms 1 and 7. *Biochemistry* **51**, 7654–7664 (2012).

- Francois-Martin, C., Rothman, J. E. & Pincet, F. Low energy cost for optimal speed and control of membrane fusion. *Proc. Natl Acad.* Sci. USA 114, 1238–1241 (2017).
- 61. Manca, F. et al. SNARE machinery is optimized for ultrafast fusion. *Proc. Natl Acad. Sci. USA* **116**, 2435–2442 (2019).

Acknowledgements

We are grateful to Drs Dimitri Kullmann, James Rothman, and Dmitri Rusakov for reading the manuscript and providing critical feedback. This work was supported by National Institute of Health (NIH) grant NS133091 (S.S.K. and K.E.V.); UKRI MRC Project Grant MR/T002786/1 (Y.T. and K.E.V.); UKRI BBSRC/NC3R Project Grant NC/X002233/1 (K.E.V.).

Author contributions

S.S.K. and K.E.V. conceived the project; D.B. and M.B. carried out the in vitro functional analysis; C.A.N. and Y.T. contributed to the implementation of the computational model; C.A.N. performed all model simulations. S.S.K. and K.E.V. wrote the manuscript. All authors discussed the results and commented on the manuscript.

Competing interests

The authors declare no competing interests.

Additional information

Supplementary information The online version contains supplementary material available at https://doi.org/10.1038/s41467-024-54960-1.

Correspondence and requests for materials should be addressed to Kirill E. Volynski or Shyam S. Krishnakumar.

Peer review information *Nature Communications* thanks the anonymous reviewers for their contribution to the peer review of this work. A peer review file is available.

Reprints and permissions information is available at http://www.nature.com/reprints

Publisher's note Springer Nature remains neutral with regard to jurisdictional claims in published maps and institutional affiliations.

Open Access This article is licensed under a Creative Commons Attribution 4.0 International License, which permits use, sharing, adaptation, distribution and reproduction in any medium or format, as long as you give appropriate credit to the original author(s) and the source, provide a link to the Creative Commons licence, and indicate if changes were made. The images or other third party material in this article are included in the article's Creative Commons licence, unless indicated otherwise in a credit line to the material. If material is not included in the article's Creative Commons licence and your intended use is not permitted by statutory regulation or exceeds the permitted use, you will need to obtain permission directly from the copyright holder. To view a copy of this licence, visit http://creativecommons.org/licenses/by/4.0/.

© The Author(s) 2024